

## Intercalation and Stitching of Graphite Oxide with Diaminoalkanes

Margarita Herrera-Alonso, Ahmed A. Abdala,<sup>†</sup> Michael J. McAllister, Ilhan A. Aksay, and Robert K. Prud'homme\*

Department of Chemical Engineering, Princeton University, Princeton, New Jersey 08544

Received June 7, 2007

The intercalation reaction of graphite oxide with diaminoalkanes, with the general formula  $\text{H}_2\text{N}(\text{CH}_2)_n\text{NH}_2$  ( $n = 4-10$ ), was studied as a method for synthesizing pillared graphite with tailored interlayer spacing. Interlayer spacings from 0.8 to 1.0 nm were tailored by varying the size of the intercalant from  $(\text{CH}_2)_4$  to  $(\text{CH}_2)_{10}$ . X-ray diffraction and infrared spectroscopy were used to confirm intercalation, and the frequency of the  $\text{CH}_2$  stretch confirmed that the intercalants are in a disordered state, with an important contribution from the *gauche* conformer. Sequential intercalation of diaminoalkanes followed by dodecylamine demonstrated the inability of these “stitched” systems to undergo expansion along the *c*-direction, indicative of cross-linking. Finally, the reaction of graphite oxide with diaminoalkanes under reflux and for extended periods ( $> 72$  h) resulted in the chemical reduction of the graphite oxide to a disordered graphitic structure.

### Introduction

Intercalation of organic molecules in the gallery spacing of layered materials is a common modification technique since the simplicity of these reactions allows facile control over the chemical and physicochemical characteristics of the derivatives.<sup>1</sup> An example of the applicability of this method is in the fabrication of polymer/clay nanocomposites, where dispersability of the inorganic platelets within the polymer matrix has a profound effect on the mechanical, thermal, and barrier properties of the resulting composite.<sup>2</sup> Organophilization of inherently hydrophilic aluminosilicates through ion-exchange reactions with alkylammonium quaternary salts results in surfaces that exhibit enhanced compatibility with hydrophobic polymers, therefore improving their dispersability.<sup>3</sup> Recently much attention has been focused on intercalation of difunctional reagents since they can lead to bridged or pillared nanostructures with potential applications as catalytic supports, selective adsorbents, and molecular vessels.<sup>4-6</sup>

Depending on the nature of the host and the intercalant, pillaring and stitching can be accomplished by three methods: (i) ion exchange between a difunctional ionic intercalant and the native ions of the host; (ii) exfoliation of the host followed by reaction with the difunctional reagent and reassembly; and (iii) intercalation of a difunctional molecule chemically anchored at one end and capable of undergoing a different reaction on the other end. Noteworthy examples of bridged systems include  $\gamma$ -zirconium phosphate bridged with *n*-alkanediphosphonic acids or polyethylene oxide,<sup>4,5</sup> montmorillonite (MMT) clay bridged by diaminoalkanes,<sup>6</sup> and graphite oxide (GO) pillared with (3-aminopropyl)trimethoxysilane or iron oxide.<sup>7,8</sup> Intercalation of a difunctional reagent, however, does not ensure bridging, since

the intercalant can also adopt a single-tail tethered conformation, where only one end of the difunctional molecule reacts, or a loop conformation, where each end interacts with the same layer.<sup>6</sup>

GO, an oxygen-rich derivative of graphite, is a layered material capable of undergoing intercalation by one-dimensional expansion along its *c*-axis. Since its first synthesis by Brodie in the 1850s,<sup>9</sup> GO has been characterized by a combination of spectroscopic techniques in order to establish a structural model that explains its chemical composition and reactivity. Although its stoichiometry depends on the method used for its preparation, it is commonly accepted that it consists of randomly distributed regions of unoxidized (aromatic) graphite and regions of aliphatic six-membered rings, rich in oxygen-containing functional groups, including epoxys and hydroxyls.<sup>10-12</sup> It is believed that the epoxy and hydroxyl functionalities lie above and below each layer, while carboxylic acid groups decorate the edges.<sup>10</sup> Oxidation, therefore, provides the otherwise unreactive graphite with functional groups that can be used as reactive handles to tailor its properties. The hydroxyl groups possess acidic protons, allowing GO to undergo intercalation through ion exchange, analogous to MMT clays.<sup>13-16</sup> However, unlike MMT, its rich surface chemistry also allows covalent bonding of the intercalant directly to the layers. Chemistries targeted at the hydroxy and epoxy functionalities have been studied previously, with the objective of assessing the reactivity of these functional groups in the intercalated structure, as well as controlling the interlayer spacing and hydrophobicity by careful consideration of the size and molecular structure of the intercalants.<sup>7,10,17-19</sup>

\* Corresponding author. E-mail: prudhom@princeton.edu.

<sup>†</sup> Current address: Department of Chemical Engineering, The Petroleum Institute, POB 2533, Abu Dhabi, United Arab Emirates.

(1) Lagaly, G. *Appl. Clay Sci.* **1999**, *15*, 1–9.  
 (2) Gleiter, H. *Adv. Mater.* **1992**, *4*, 474–481. Novak, B. M. *Adv. Mater.* **1993**, *5*, 422–433. Pinnavaia, T. J.; Lan, T. *Chem. Mat.* **1994**, *6*, 2216–2219.  
 (3) Yano, K.; Usuki, A.; Okada, A.; Kurauchi, T.; Kamigaito, O. *J. Polym. Sci., Part A: Polym. Chem.* **1993**, *31*, 2493–2498.  
 (4) Messersmith, P. B.; Giannelis, E. P. *Chem. Mat.* **1994**, *6*, 1719–1725.  
 (5) Alberti, G.; Mascarós-Murcia, S.; Viviani, R. *J. Am. Chem. Soc.* **1998**, *120*, 9291–9295.  
 (6) Alberti, G.; Brunet, E.; Dionigi, C.; Juanes, O.; de la Mata, M. J.; Rodríguez-Ubis, J. C.; Viviani, R. *Angew. Chem., Int. Ed.* **1999**, *38*, 3351–3353.  
 (7) Ha, B.; Char, K. *Langmuir* **2005**, *21*, 8471–8477.

(7) Bourlinos, A. B.; Gournis, D.; Petridis, D.; Szabó, T.; Szeri, A.; Dékány, I. *Langmuir* **2003**, *19*, 6050–6055.

(8) Morishige, K.; Hamada, T. *Langmuir* **2005**, *21*, 6277–6281.

(9) Brodie, B. C. *Philos. Trans. R. Soc. London* **1859**, *149*, 249.

(10) Lorf, A.; He, H.; Forster, M.; Klinowski, J. *J. Phys. Chem. B* **1998**, *102*, 4477–4482.

(11) Mermoux, M.; Chabre, Y.; Rousseau, A. *Carbon* **1991**, *29*, 469–474.

(12) Hontoria-Lucas, C.; López-Peinado, A. J.; López-González, J. de D.; Rojas-Cervantes, M. L.; Martín-Aranda, R. M. *Carbon* **1995**, *33*, 1585–1592.

(13) Liu, Z.-H.; Wang, Z.-M.; Yang, X.; Ooi, K. *Langmuir* **2005**, *18*, 4926–4932.

(14) Matsuo, Y.; Niwa, T.; Sugie, Y. *Carbon* **1999**, *37*, 897–901.

(15) Matsuo, Y.; Watanabe, K.; Fukutsuka, T.; Sugie, Y. *Carbon* **2003**, *41*, 1545–1550.

(16) Dékány, I.; Krüger-Grasser, R.; Weiss, A. *Colloid Polym. Sci.* **1998**, *276*, 570–576.

(17) Matsuo, Y.; Fukunaga, T.; Fukutsuka, T.; Sugie, Y. *Carbon* **2004**, *42*, 2113–2130.

An interesting and potentially important application of pillared graphitic materials is in the area of hydrogen storage. Recent theoretical calculations indicate that confinement effects should have a major impact on hydrogen storage between graphite sheets.<sup>20</sup> Simulations show that there exists an optimal combination of pressure and pore geometry (interlayer distance) that maximizes the storage capacity.<sup>20</sup> Furthermore, chemical substitution disrupts the planarity of the graphene sheets and creates a distorted surface, which has been referred to as “puckered”<sup>21</sup> or “roughened”.<sup>22</sup> The combination of altered aromaticity, bond distortion, and local coordination changes arising from the distorted surface, cause an increase in the polarizability of graphene. Binding energies for hydrogen range from 52 meV in a honeycomb graphene structure to 75 meV in a model system containing Stone–Wales defects.<sup>22</sup> Pillaring of the graphitic sheets would be necessary to maintain the optimal separation between graphite layers and to resist delamination of the layered structure during pressure cycling of a hydrogen storage medium.

The present work describes a detailed study of the intercalation reaction of  $\alpha,\omega$ -diaminoalkanes with GO to produce chemically bridged derivatives. The size of the intercalant was systematically varied to determine its effect on the interlayer spacing, and the conformation of the intercalant in the layered structure was assessed by swelling experiments.

### Experimental Section

**Materials.** All materials were used as received. Graphite particles (40  $\mu\text{m}$  particle size) were provided by Asbury Carbon, New Jersey. Sulfuric acid (98%), hydrochloric acid (37%), and nitric acid (fuming, 90%) were purchased from Fisher. Potassium chlorate, ethanol (reagent grade), diaminoalkanes, and alkylamines were obtained from Aldrich.

**Graphite Oxide.** GO was synthesized from natural flake graphite (40  $\mu\text{m}$  particle size) by the Staudenmaier method.<sup>23</sup> Sulfuric acid (160 mL) and nitric acid (90 mL) were added to a round-bottom flask, containing a stir bar, and cooled with an ice bath for 1 h. Graphite particles (10 g) were added to the acids mixture under vigorous stirring, and the suspension was cooled for 20 min. Potassium chlorate (110 g) was slowly added over 15 min, while keeping the reaction vessel inside an ice bath, making sure that the temperature did not exceed 35 °C. *Caution!* This reaction results in the formation of chlorine dioxide gas, which is explosive at high concentrations.<sup>24</sup> To minimize the risk of explosion it is recommended that the addition of potassium chlorate be done slowly while monitoring the temperature. Oxidation was allowed to proceed for 96 h. The suspension was washed with an aqueous hydrochloric acid solution (10 vol %) to remove the sulfate ions and then washed repeatedly with deionized (DI) water until neutral pH. The final concentration of GO in the suspension was approximately 6 mg GO/mL.

**Intercalation of Graphite Oxide with Mono- and Difunctional Amines.** In a typical experiment, 1,8-diaminooctane (600 mg) was dissolved in ethanol (35 mL) and added dropwise to a suspension of GO in water (200 mg GO, 33 mL) under vigorous stirring. The

reaction continued for 24 h at room temperature or under reflux (78 °C). Intercalated GO was isolated by centrifugation and thoroughly washed with 1:1 ethanol/water (45 mL, 4 $\times$ ), filtered, and dried at 80 °C under vacuum for a minimum of 12 h prior to characterization. Reactions with alkylamines  $\text{CH}_3(\text{CH}_2)_n\text{NH}_2$  ( $n = 4\text{--}12$ ) or diaminoalkanes  $\text{H}_2\text{N}(\text{CH}_2)_n\text{NH}_2$  ( $n = 4\text{--}10$ ) were conducted following the same procedure.

**Characterization.** X-ray diffraction (XRD) patterns were acquired on a Rigaku MiniFlex diffractometer with  $\text{Cu K}\alpha$  radiation. Simultaneous thermogravimetric analysis (TGA) and differential scanning calorimetry (DSC) experiments were conducted with a Netzsch STA 449C thermal analyzer. Analyses were done under a nitrogen atmosphere (50 mL/min flow rate) at a heating rate of 1 °C/min. Fourier transform infrared spectroscopy (FTIR) was performed on a Thermo Nicolet 6700 FT-IR spectrometer. GO and its derivatives were thoroughly ground, mixed with potassium bromide to a final concentration of approximately 0.15 wt %, and pressed into pellets. Elemental analysis was performed by Atlantic Microlab Inc., Norcross GA.

### Results and Discussion

**Graphite Oxide Characterization.** GO was characterized by elemental analysis, <sup>13</sup>C NMR, XPS, and FTIR. Results from XPS and elemental analysis were discussed in a previous publication.<sup>25</sup> Briefly, the chemical composition of GO determined by elemental analysis was  $\text{C}_8\text{O}_{4.3}\text{H}_{3.6}$ , while the C/O ratio calculated from XPS was 2.6. High-resolution  $\text{C}_{1s}$  XPS (Figure 1, Supporting Information) showed signals characteristic of graphitic carbon (C–C, 284.6 eV) and carbon singly bound to oxygen (C–O, 286.6 eV), either as epoxy or hydroxyl.<sup>12,26</sup> The broad  $\text{O}_{1s}$  spectrum is also indicative of the presence of more than one oxygen-containing species: oxygen in carboxyls (531.3 eV),  $\text{C}_{\text{aliphatic}}\text{--O}$  (532.6 eV), and  $\text{C}_{\text{aromatic}}\text{--O}$  (531.1 eV).<sup>12</sup> Solid-state <sup>13</sup>C NMR results (Figure 2, Supporting Information) are in agreement with the XPS data. The spectrum contains two distinguishable peaks at chemical shifts ( $\delta$ ) of 60–70 and 133 ppm. The signal between 60 and 70 ppm is composed of two peaks, which have been assigned to hydroxyl (70 ppm) and 1,2-epoxy groups (60 ppm). The peak at 133 ppm corresponds to  $\text{sp}^2$ -hybridized carbon. The third signal, observed at lower fields (210–220 ppm), has been assigned to spinning side bands of the unsaturated carbons.<sup>11</sup> The NMR spectrum is in qualitative agreement with the model proposed by Lerf et al.<sup>10</sup> FTIR analysis of GO is discussed in more detail further in the text.

**Intercalation of Graphite Oxide with  $\alpha,\omega$ -Diaminoalkanes.** The rich surface chemistry of GO allows for covalent modification by reactions at hydroxy and epoxy groups. An example is the intercalation reaction of GO with monofunctional amines, which proceeds by nucleophilic substitution on the epoxy groups, provided that the amines are in neutral form.<sup>7,10</sup> It is possible then, that intercalation of a difunctional amine could produce a pillared structure, as shown in Figure 1.

For this, GO was reacted with a series of  $\alpha,\omega$ -diaminoalkanes that differ in the number of methylene units ( $n$ ) separating the terminal amine groups. XRD patterns of GO and the intercalated derivatives are shown in Figure 2. A gradual increase in the basal spacing of GO is observed as the hydrocarbon chain length of the diamine increases from  $n = 4$  to  $n = 10$ , suggesting that intercalation takes place and that the interlayer spacing is sensitive to the size of the intercalant.

(18) Valerga Jiménez, P.; Arufe Martínez, M. I.; Martín Rodríguez, A. *Carbon* **1985**, *23*, 473–479.

(19) Aragón, F.; Ruíz, J. C.; MacEwan, D. M. C. *Nature* **1959**, *183*, 740–741.

(20) Wang, Q.; Johnson, J. K. *J. Chem. Phys.* **1999**, *110*, 577–586. Wang, Q.; Johnson, J. K. *J. Phys. Chem. B* **1999**, *103*, 277–281. Kowalczyk, P.; Tanaka, H.; Holyst, R.; Kaneko, K.; Ohmori, T.; Miyamoto, J. *J. Phys. Chem. B* **2005**, *109*, 17174–17183. Rzepka, M.; Lamp, P.; de la Casa-Lillo, M. A. *J. Phys. Chem. B* **1998**, *102*, 10894–10898.

(21) Boehm, H. P.; Setton, R.; Stumpp, E. *Pure Appl. Chem.* **1994**, *66*, 1893–1901.

(22) Pradhan, B. K.; Harutyunyan, A. R.; Stojkovic, D.; Grossman, J. C.; Zhang, P.; Cole, M. W.; Crespi, V.; Goto, H.; Fujiwara, J.; Eklund, P. C. *J. Mater. Res.* **2002**, *17*, 2209–2216.

(23) Staudenmaier, L. *Ber. Dtsch. Chem. Ges.* **1898**, *31*, 1481–1487.

(24) López, M. I.; Croce, A. E.; Sicre, J. E. *J. Chem. Soc., Faraday Trans.* **1994**, *90*, 3391–3396.

(25) Schniepp, H. C.; Li, J.-L.; McAllister, M. J.; Sai, H.; Herrera-Alonso, M.; Adamson, D. H.; Prud'homme, R. K.; Car, R.; Saville, D. A.; Aksay, I. A. *J. Phys. Chem. B* **2006**, *110*, 8535–8539.

(26) Xing, Y. C.; Li, L.; Chusuei, C. C.; Hull, R. V. *Langmuir*. **2005**, *21*, 4185–4190. de la Puente, G.; Pis, J. J.; Menendez, J. A.; Grange, P. *J. Anal. Appl. Pyrolysis* **1997**, *43*, 125–138.

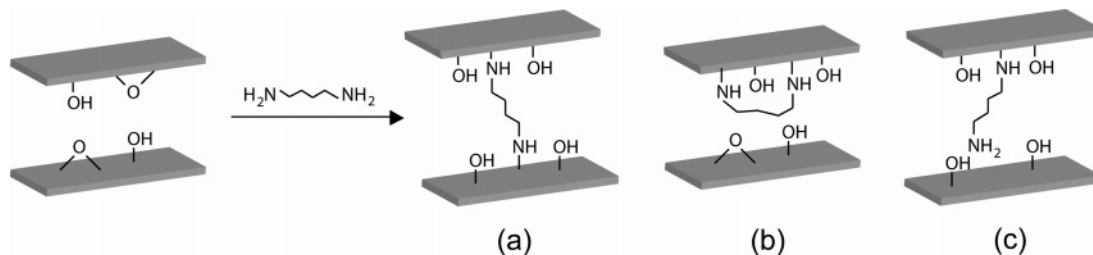


**Figure 1.** Schematic representation of the intercalation reaction of a diaminoalkane in the interlayer spacing of GO, showing the intercalant in a bridge conformation (a), loop conformation (b), and tail conformation (c).

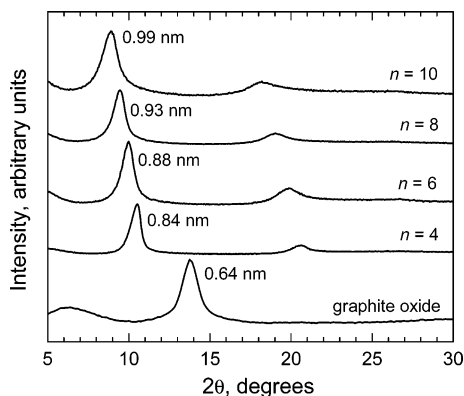


**Figure 2.** X-ray diffraction patterns of GO and GO intercalated with diaminoalkanes with the general formula  $\text{H}_2\text{N}(\text{CH}_2)_n\text{NH}_2$ , showing the dependence of the length of the intercalant on interlayer spacing. Intercalations were conducted at room temperature.

Pillared structures composed of planar sheets separated by alkylamines with extended conformations ( $l_{\text{max}} = 0.154 + 0.1265n$ ),<sup>27</sup> having a tetrahedral angle between the alkylamine and GO of  $\theta = 54^\circ$  would produce gallery spacing  $d_{002} = l_{\text{max}} \sin \theta$ . However, the oxidation of the originally planar graphite results in puckered sheets, which are no longer coplanar. Atomic force microscopy (AFM) and first-principles atomistic modeling studies have shown that the undulations in the graphene sheets are on the order of  $\sim 0.2\text{--}0.4$  nm.<sup>25</sup> The separation from the native 0.34-nm spacing for graphite to the 0.64 nm for GO is a consequence of this puckering. The projected distance of the tethered chain is then a function of the local orientation of the GO surface. Therefore, there is no method to predict *a priori* the increase in interlayer spacing with intercalation. Furthermore, the theoretical prediction is based on the alkyl chain being in an all-*trans* (chain-extended) conformation, which is the less prevalent conformation in intercalation studies. Experimental results and theoretical predictions of the interlayer spacing (i.e.,  $d_{002} = l_{\text{max}} \sin \theta$ , where  $l_{\text{max}}$  is calculated as shown above) are presented in Figure 3. The difference between our results and those obtained from the theoretical prediction are explained in terms of the conformational ordering of the alkyl chains, which have an important *gauche* component as determined by FTIR. These results are also in contrast with those obtained for the intercalation of GO with aminoacids ( $\text{H}_2\text{N}(\text{CH}_2)_n\text{COO}^- \text{Na}^+$  with  $n = 1$  and  $n = 7$ ), where no change in the  $d$ -spacing was observed, regardless of the length of the hydrocarbon segment separating the functional groups.<sup>7</sup> The progressive change in  $d$ -spacing (Figure 2) demonstrates intercalation but does not prove stitching between layers.

It was previously reported that the reaction of GO with long-chain alkylamines ( $n = 16$ ) was kinetically favored at higher

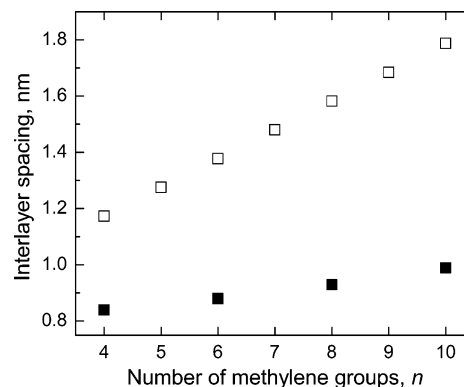


**Figure 3.** Interlayer spacing of intercalated GO as a function of the length of the alkyl chain for diaminoalkanes (■) and values predicted for alkylamines in the maximum extended conformation, given by:  $d = (0.154 + 0.1265n) \sin \theta$  (□).

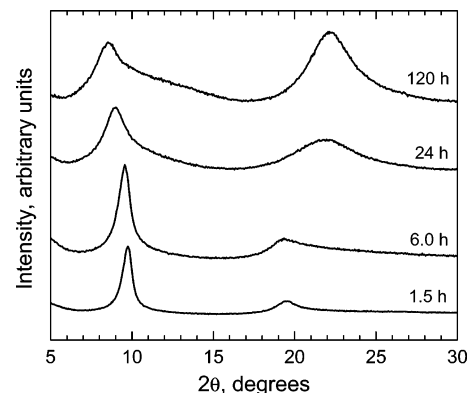


**Figure 4.** X-ray diffraction patterns of GO intercalated with diaminoctane under reflux for different reaction times. The peak that develops between  $20.5^\circ\text{--}23^\circ$  is ascribed to turbostratic graphite, product of the chemical reduction of GO.

reaction temperatures and for long reaction times (24 h) due to steric reasons.<sup>7</sup> We anticipated that this would have an effect on the reactions with difunctional intercalants because of their reduced mobility once anchored on one end; therefore, we studied intercalation under reflux ( $78^\circ\text{C}$ ) for varying periods of time (2–72 h). The results for all diaminoalkanes studied were similar, and therefore we limit the discussion to the reaction with diaminoctane. While only a small change in the position of the principal reflection is observed with reaction time, the most striking difference is the intensity of the peak observed between  $2\theta = 20.5^\circ\text{--}23^\circ$ , corresponding to an average interlayer spacing of  $\sim 0.4$  nm (Figure 4). This broad reflection is assigned to disordered graphitic platelets (turbostratic graphite),<sup>28</sup> demonstrating that chemical reduction of GO takes place under these

(27) Israelachvili, J. *Intermolecular and Surface Forces*; Academic Press: London, 1992.

(28) Dresselhaus, M. S. In *Supercarbon: Synthesis, Properties and Applications*; Yoshimura, S., Chang, R. P., Eds. Springer Series in Materials Science, Vol. 33; Springer: New York, 1998.

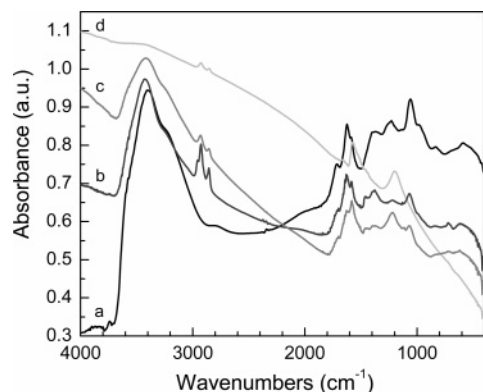


**Figure 5.** FTIR spectra of GO (a), GO/octylamine (b), GO/diaminooctane at room temperature (c), GO/diaminooctane under reflux (d). The intercalation of mono- and difunctional amines is evidenced by the appearance of methylene bands (2800–3000  $\text{cm}^{-1}$ ).

conditions. It is important to mention that this reaction was observed only in the presence of the diamine. While the mechanism for this unexpected reaction is unknown, we suspect that it could be attributed to the presence of trace amounts of metals in the diamine (purity  $\sim 95\%$ ), consistent with the deoxygenation of aromatic alcohols in refluxing 2-propanol and Raney nickel catalyst.<sup>29</sup>

Infrared spectroscopy was also used to confirm intercalation; FTIR spectra of GO and its derivatives are presented in Figure 5. The spectrum of GO is in good agreement with previous work.<sup>11,12,30</sup> The intense band at 3408  $\text{cm}^{-1}$  and the broad band at 3200  $\text{cm}^{-1}$  are attributed to stretching of the O–H bond of CO–H and water, respectively. The band at 1700  $\text{cm}^{-1}$  is associated with stretching of the C=O bond of carbonyl or carboxyl groups. The bands present at 1630 and 1383  $\text{cm}^{-1}$  are attributed to deformations of the O–H bond in water and CO–H groups, respectively. Deformation of the C–O bond is observed as the intense band present at 1057  $\text{cm}^{-1}$ . The FTIR spectra of GO intercalated with octylamine, as reference, and diaminooctane (at room temperature) differ from that of GO in the signals observed at 1470, 1570, 2924, and 2852  $\text{cm}^{-1}$ . The first two peaks are assigned to the bending vibration (scissoring) of  $-\text{CH}_2-$ , and vibration of the N–H groups of the intercalants, respectively. The strongest signals, observed at higher frequencies, are attributed to asymmetric (2924  $\text{cm}^{-1}$ ) and symmetric (2852  $\text{cm}^{-1}$ ) stretching of the methylene group of the alkylamines (spectra b and c of Figure 5). Similar results were observed for intercalants with  $4 < n < 10$ . The higher intensity of these bands for the monofunctional vs the difunctional amine is indicative of a larger amount of intercalated material for the former case.

Detailed studies on the intercalation of alkylamines in the interlayer spacing of MMT clays revealed that the frequency and intensity of the bending mode ( $\delta$ ), and asymmetric ( $\nu_{\text{as}}$ ) and symmetric ( $\nu_{\text{s}}$ ) stretching modes of the  $\text{CH}_2$  group are sensitive to the conformation and packing arrangement of the alkyl chains in confined environments.<sup>6,31–33</sup> Interchain interactions and packing arrangements can be inferred from the intensity and shape of the bending vibration, observed between 1466 and 1472  $\text{cm}^{-1}$ . Higher frequencies are indicative of all-*trans* chains

in a crystalline state. Increased chain motion, associated with a less-ordered liquid-like state, leads to peak broadening and decreased intensities. On the other hand, chain conformation (*gauche/trans* ratio) can be estimated from the asymmetric stretching bands with frequencies ranging from 2937 to 2919  $\text{cm}^{-1}$ . In general, a shift in  $\nu_{\text{as}}(\text{CH}_2)$  from a lower frequency, indicative of highly ordered all-*trans* systems, to a higher value, is observed as the number of *gauche* conformers, and thus the disorder, increases. The reported value of  $\nu_{\text{as}}$  for fully stretched chains was 2919  $\text{cm}^{-1}$ ,<sup>31</sup> while the most disordered system with the highest *gauche/trans* conformer ratio was observed at 2937  $\text{cm}^{-1}$ .<sup>6,32</sup> Bending and asymmetric stretching of the methylene group of GO intercalated with diaminooctane and octylamine occurs at  $\delta = 1467 \text{ cm}^{-1}$  and  $\nu_{\text{as}} = 2929 \text{ cm}^{-1}$ , and  $\delta = 1466 \text{ cm}^{-1}$  and  $\nu_{\text{as}} = 2926 \text{ cm}^{-1}$ , respectively. Compared to reference values, the broadness of the bending signal, in combination with the peak position of the asymmetric stretching suggests that the intercalants are in a disordered state, with an important contribution from the *gauche* conformer. This observation also explains the difference between the experimental and theoretical interlayer spacing (Figure 3), as the premise of a chain-extended conformation is not applicable. Furthermore, the difference in  $\nu_{\text{as}}$  peak positions between the difunctional and monofunctional intercalants suggests a higher degree of conformational order for the monofunctional case.

The spectrum of GO intercalated with diaminoalkanes under reflux for an extended period (72 h) is essentially featureless and markedly different from that of its precursor. The signals characteristic of oxygen-containing functionalities are lost, and two new signals, at 1572 and 1199  $\text{cm}^{-1}$  appear (Figure 5d). This spectrum is reminiscent of pristine graphite, which has two IR-active modes: a signal at 1571  $\text{cm}^{-1}$ , attributed to the in-plane  $E_{1u}$  mode, and a signal at 868  $\text{cm}^{-1}$ , assigned to the out-of-plane  $A_{2u}$  mode.<sup>34–37</sup> The latter signal is not observed in the spectra presented in Figure 5 since it is generally of lower intensity and difficult to observe. The signal at 1571  $\text{cm}^{-1}$  shows broadening toward lower energy, which has been attributed to increased disorder, bending of the graphite sheets, and a change in the interplanar bonding.<sup>36</sup> The peak at 1194  $\text{cm}^{-1}$  was previously observed for chemical vapor-deposited single-wall carbon nanotubes; however, it has not yet been identified.<sup>37</sup> These results support those from XRD in that, while intercalation of the difunctional amines occurs, more vigorous reaction conditions result in the chemical reduction of GO. This suggests that reduction produces a collapse from the original 0.68 nm GO spacing to turbostratic graphite with  $\sim 0.4$  nm spacing.

The thermal behavior of GO and its derivatives was studied by TGA/DSC (Figure 6). GO, hydrophilic because of its high concentration of polar functional groups, exhibits two regions of mass loss. The first occurs at temperatures below 125  $^{\circ}\text{C}$  and is attributed to loss of adsorbed water ( $\sim 4\%$ ). The second occurs at an onset temperature of 150  $^{\circ}\text{C}$  and is associated with the thermal decomposition of oxygen-containing functionalities to generate carbon dioxide and water.<sup>7,13,30,38</sup> The corresponding DSC shows a large exothermic signal with a peak at 210  $^{\circ}\text{C}$ . The curve slowly plateaus around 300  $^{\circ}\text{C}$ , with a total mass loss of

(29) Gross, B. H.; Mebane, R. C.; Armstrong, D. L. *Appl. Catal., A* **2001**, *219*, 281–289.

(30) Kovtyukhova, N. I.; Olliver, P. J.; Martin, B. R.; Mallouk, T. E.; Chizhik, S. A.; Buzaneva, E. V.; Gorchinskiy, A. D. *Chem. Mater.* **1998**, *11*, 771–778.

(31) Vaia, R. A.; Teukolsky, R. K.; Giannelis, E. P. *Chem. Mater.* **1994**, *6*, 1017–1022.

(32) Li, Y.; Ishida, H. *Langmuir* **2003**, *19*, 2479–2484.

(33) Xie, W.; Gao, Z.; Pan, W.-P.; Hunter, D.; Singh, A.; Vaia, R. *Chem. Mater.* **2001**, *13*, 2979–2990.

(34) Friedel, R. A.; Carlson, G. L. *J. Phys. Chem.* **1971**, *75*, 1149–1151.

(35) Conrad, M. P.; Strauss, H. L. *Phys. Rev. B* **1985**, *31*, 6669–6675.

(36) Kastner, J.; Pichler, T.; Kuzmany, H.; Curran, S.; Blau, W.; Weldon, D. N.; Delamaisiere, M.; Draper, S.; Zandbergen, H. *Chem. Phys. Lett.* **1994**, *221*, 53–58.

(37) Zhang, J.; Zou, H.; Qing, Q.; Yang, Y.; Li, Q.; Liu, Z.; Guo, X.; Du, Z. *J. Phys. Chem. B* **2003**, *107*, 3712–3718.

(38) McAllister, M. J.; Li, J.-L.; Adamson, D. H.; Schniepp, H. C.; Abdala, A. A.; Liu, J.; Herrera-Alonso, M.; Milius, D. L.; Car, R.; Prud'homme, R. K.; Aksay, I. A. *Chem. Mater.* Published online May 25, 2007, <http://dx.doi.org/10.1021/cm0630800>

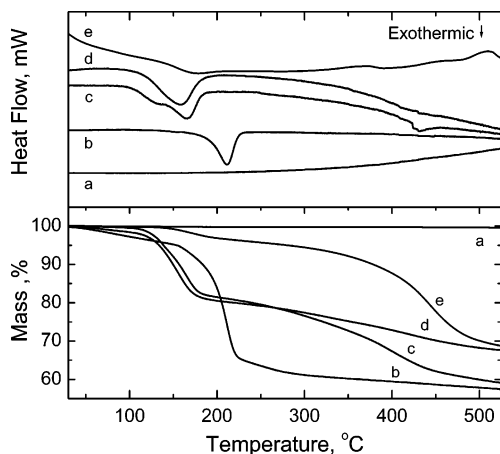


**Figure 6.** DSC (top) and TGA (bottom) thermograms of: (a) graphite, (b) GO, (c) GO intercalated with octylamine, (d) GO intercalated with diaminoctane at room temperature and (e) under reflux.

44%. GO intercalated with octylamine and diaminoctane (Figure 6) exhibits loss of oxygen-containing functionalities at 125 °C (vs 150 °C onset observed for GO), which accounts for approximately 18% of the total mass. It is unlikely that the octylamine or diaminoctane would decompose within this temperature range since their boiling temperatures are 175 and 226 °C, respectively. The decreased mass loss within the temperature range of 125–210 °C for the intercalated derivatives, compared to the mass of GO, is attributed to loss or transformation of some oxygen-containing groups either by reaction with amines (ring-opening of epoxides) or by chemical reduction. Decomposition of the intercalant occurs between 300 and 475 °C and is accompanied by an exothermic signal at 425 °C, more clearly observed for the reaction with octylamine. While the final mass loss of the sample intercalated with the diaminoctane appears to be lower than the others, the variability in the data ( $\pm 7\%$ ) does not allow conclusions to be made at this point.

The thermogram of GO intercalated with diaminoctane under reflux is very different from those discussed previously (Figure 6). A negligible mass loss was observed below 210 °C ( $\sim 5\%$ ), supporting the results from FTIR and XRD, which suggest that chemical reduction takes place under these conditions. While thermal decomposition of the intercalant occurs between 300 and 475 °C, based on the magnitude of the decrease it is not expected to account for the total mass loss observed within this range. The turbostratic graphitic material produced is less thermally stable than natural flake graphite, and some of the mass loss may be due to thermal decomposition at these temperatures.

**Cross-Linking.** As suggested by He et al. for the reaction of GO with hexamethylenediisocyanate, when a bifunctional molecule intercalates and reacts with GO, it can do so by attachment at two sites on the same layer, forming rings, or by reacting at sites on adjacent layers, forming bridges.<sup>39</sup> More recently, Ha and Char showed that 1,12-diaminododecane could adopt different conformations inside the galleries of MMT clay by varying the pH during intercalation.<sup>6</sup> In both cases, swelling experiments were used as indirect methods to assess cross-linking. We employed the same strategy to demonstrate the formation of interlayer stitching. If the diaminoalkane bridges adjacent layers, the cross-links should resist swelling by solvents. Our XRD results for the sequential intercalation of dodecylamine

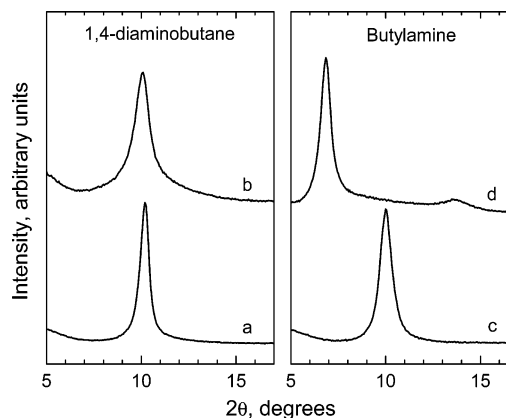


**Figure 7.** XRD data on swelling experiments of GO intercalated with difunctional (left) and monofunctional amines (right). The example shown corresponds to a sequential intercalation with 1,4-diaminobutane (a) and butylamine (c) followed by dodecylamine (b) and (d).

into alkylamine- and diaminoalkane-intercalated GO show that this is the case (Figure 7).

The diffraction pattern on the left in Figure 7 corresponds to a sample that was intercalated with a difunctional amine, while the sample on the right was intercalated with a monofunctional amine. Intercalation of dodecylamine into GO reacted with butylamine produced an increase in the *d*-spacing to approximately 1.40 nm. Although this value is lower than the *d*-spacing of dodecylamine-intercalated GO (1.72 nm), it serves as a proof-of-concept for the expansion of an unconstrained system along the *c*-axis. On the other hand, systems that were initially reacted with difunctional amines, in this case diaminobutane, showed a very small change in the interlayer spacing after the second intercalation. This result can be explained by considering that (i) the second intercalation did not occur because of a decreased number of reaction sites or (ii) the system was cross-linked and, therefore, restricted to expansion. The composition of GO, estimated by elemental analysis, is approximately  $C_8O_{4.3}H_{3.6}$ . Considering that the composition of oxygen-containing functional groups in GO is similar to the structural model proposed by Lerf (C–O–C, 41%; C–OH, 32%, –COOH, 26%), the  $NH_2/epoxy$  ratio would be 3.3 and 6.6 for the reaction with butylamine and 1,4-diaminobutane, respectively. Given that there is an excess of amines with respect to the number of epoxys in both cases and that the reactivity of the amines is equivalent, it is unlikely that there would be more unreacted sites for the intercalation of a monofunctional vs a difunctional amine. We therefore conclude that the lack of swelling after reaction with diamines is evidence for the existence of stitching between GO sheets.

## Conclusions

The present work discusses the intercalation reaction of GO with diaminoalkanes. XRD analysis revealed that the interlayer spacing was dependent on the size of the intercalant. Diaminoalkanes with 4–10 methylene groups produce 0.8- and 1.0-nm interlayer spacings, which correspond to the values that should be most beneficial for hydrogen storage in graphitic stacks.<sup>20</sup> These results were complemented by infrared analysis, where the shift of the methylene groups revealed that the intercalant was in a disordered conformation, with a strong contribution from the *gauche* conformer. Swelling experiments by sequential intercalation showed that the reaction of GO with diaminoalkanes produces a pillared structure with constrained gallery spacing. In contrast, GO reacted with monoamines produced layered

(39) He, H.; Riedl, T.; Lerf, A.; Klinowski, J. *J. Phys. Chem.* **1996**, *100*, 19954–19958.

structures that swelled upon the addition of larger intercalants. We believe this demonstrates the successful stitching (or cross-linking) across layers to produce pillared structures. Reaction of GO with diaminoalkanes under more rigorous conditions resulted in chemical reduction to a disordered graphitic structure, evidenced by XRD and FTIR.

The stitched, layered structures produced should be attractive materials for polymer composite applications. Cross-linking between sheets should eliminate problems associated with graphene sliding that leads to poor mechanical properties with conventional GO-filled composites.<sup>40</sup> Further, the observation that under relatively mild reaction conditions the stitched graphitic

sheets can be reduced enhances their potential as a hydrogen storage media. The combination of defined 1-nm interlayer spacing and reduction to a graphitic structure with defects causing puckering is predicted to maximize hydrogen storage.

**Acknowledgment.** Financial support from the NASA University Research, Engineering, and Technology Institute (URETI) on BioInspired Materials (BIMat) under Award No. NCC-1-02037 and the National Science Foundation NIRT under Grant No. CMS-0609049 is greatly appreciated.

**Supporting Information Available:** High-resolution C<sub>1s</sub> XPS, solid state <sup>13</sup>C NMR spectra, and experimental details. This material is available free of charge via the Internet at <http://pubs.acs.org>.

---

(40) Wang, W.-P.; Pan, C.-Y. *Polym. Eng. Sci.* **2004**, *44*, 2335–2339.